npj | parkinson's disease

Article

Published in partnership with the Parkinson's Foundation

https://doi.org/10.1038/s41531-025-01005-z

Complement C4 exacerbates astrocyte-mediated neuroinflammation and promotes α-synuclein pathology in Parkinson's disease

Wenkai Zou[1,2], Liang Kou[1,2], Yiming Wang[1,2], Zongjie Jin[1], Nian Xiong[1], Tao Wang[1] ✉ & Yun Xia[1] ✉

Complement C4, implicated in neuroinflammation and synaptic dysfunction, plays a poorly defined role in Parkinson's disease (PD). Here, we demonstrate elevated C4 levels in PD patient plasma and the substantia nigra of α-synuclein preformed fibril (α-syn PFF)-injected mice, correlating with disease severity. α-syn PFF treatment induces complement C4 expression, particularly in neurons, with astrocytes further enhancing this response. Complement C4 was found to amplify astrocytic inflammatory responses, leading to increased neuronal apoptosis and synaptic damage. Additionally, conditioned media from astrocytes treated with α-syn PFF and complement C4 accelerated α-syn aggregation and synaptic loss in cultured neurons. In vivo, complement C4 exacerbated motor dysfunction, dopaminergic neuronal loss, and α-syn pathology in α-syn PFF-injected mice. These findings reveal that complement C4 significantly contributes to the neuroinflammatory environment and α-syn pathology in PD, highlighting its potential as a therapeutic target for mitigating neurodegeneration in this disorder.

Complement is an essential component of the innate immune defense against pathogens and is critical for the efficient processing of immune complexes. The complement system is widely distributed in serum, tissue fluids, and on the surfaces of various cells. Comprising more than 30 components, this precisely regulated protein reaction system can be activated through the classical pathway, lectin pathway, or alternative pathway. These pathways initiate a series of enzyme-catalyzed reactions leading to the assembly of convertases, which in turn drive the activation of complement components. This process ultimately results in the formation of the membrane attack complex on the surface of target cells, mediating cell lysis[1]. In addition to this lytic function, active complement fragments generated during the cascade reaction mediate various biological functions. For example, complement C3b and C4b can bind to the surfaces of bacteria and other antigens, facilitating opsonization through complement receptors on target cells[1]. Meanwhile, complement C3a, C4a, and C5a can bind to receptors on basophils and other cells, thereby mediating local inflammatory responses[1].

Synucleinopathies are characterized by the accumulation of misfolded α-syn in neurons (forming Lewy bodies) and oligodendrocytes (termed glial cytoplasmic inclusions). Synucleinopathies are broadly divided into two categories: Lewy body diseases, which include Parkinson's disease (PD) and dementia with Lewy bodies (DLB), and the multiple system atrophy (MSA) group[2]. The accumulation of α-Syn leads to the gradual loss of neurons in the basal ganglia of patients, and the presence of reactive microglia in the areas of neuronal loss indicates that neuroinflammation is a core feature[3]. Some studies have investigated complement levels in the cerebrospinal fluid or blood of patients with synucleinopathies. The results indicate that patients with MSA have consistently lower levels of C3 in their cerebrospinal fluid and serum compared to control groups, whereas C3 levels in PD patients do not decrease[4]. Other studies have suggested that higher baseline levels of C3 and C4 in longitudinal biomarker studies of PD predict a poorer prognosis[5]. Proteomics analysis has identified complement Factor H as one of the most significantly altered proteins in PD, and C9 is closely associated with disease state, cognitive decline, and motor symptoms[6,7]. Furthermore, multiple immunohistochemistry (IHC) studies on postmortem brains of PD and DLB cases have shown that complement proteins and activation products are associated with hallmark lesions. C1q and activation markers iC3b, C3d, and C4d are localized to Lewy bodies (LBs) in dopaminergic neurons of the substantia nigra[8–11]. Additionally, activated microglia are closely associated with C1q/C4d-positive LBs in dopaminergic neurons[8,9].

[1]Department of Neurology, Union Hospital, Tongji Medical College, Huazhong University of Science and Technology, Wuhan, China. [2]These authors contributed equally: Wenkai Zou, Liang Kou, Yiming Wang. ✉e-mail: wangtaowh@hust.edu.cn; xiayun19931993@163.com

As the core pathological protein in PD, α-syn can activate the classical complement pathway, and the complement system is involved in α-synuclein-dependent cytotoxicity[12]. Specifically, α-syn activates the classical pathway by binding to C1q via its carboxyl terminus and is opsonized by C4b[12]. Microglia mediate the clearance of this opsonized fibrillar α-syn through phagocytic receptors CR3 and CR4, selectively binding to it[13]. In mice, the knockout of CR3 prevents neurodegeneration in the rotenone model[14]. However, preventing complement activation by knocking out C1q or C3 does not reduce neurodegeneration in the MPTP-induced PD model[15,16]. In conclusion, the mechanisms by which the complement system participates in α-syn-induced neurodegeneration remain unclear. However, these findings suggest that the complement system is a critical component in the disease progression and holds potential as a therapeutic target for synucleinopathies.

In recent years, increasing evidence has shown that the core complement component C4 plays an important role in the pathological mechanisms of neurological diseases. Levels of C4 in the cerebrospinal fluid of Alzheimer's disease (AD) patients are significantly higher compared to healthy controls, and C4 is also notably elevated in the cerebrospinal fluid of patients with schizophrenia[17,18]. Human genome analysis has revealed that increased expression of the C4 gene is significantly associated with an increased risk of schizophrenia[19]. Additionally, the increased expression of C4 in the human brain is closely associated with enhanced phagocytic activity of microglia and exacerbated synaptic loss[19]. To explore the role of component C4 in the pathogenesis of PD, we investigated the changes in complement C4 levels in PD animal and cell models, as well as its specific impact on α-syn aggregation, neuroinflammation, and PD pathological progression.

Table 1 | Clinical characteristics of patients

Subject no.	Age(years)	Gender(M/F)	Disease Duration	UPDRS-III scores	Hoehn & Yahr
1	64	M	5	24	**2**
2	58	F	9	32	2
3	63	M	8	22	2
4	66	F	5	22	2
5	67	F	5	31	2
6	68	F	6	22	2
7	67	M	5	28	2
8	80	M	7	31	2
9	64	M	7	30	2
10	58	F	5	21	2
11	66	M	5	24	3
12	70	M	6	45	3
13	72	M	8	40	3
14	76	M	8	45	3
15	78	F	7	55	3
16	63	M	10	28	3
17	78	M	7	46	3
18	72	F	6	41	3
19	67	M	10	28	3
20	64	M	9	36	3
21	68	M	14	49	3
22	76	F	15	42	3
23	81	M	8	32	3
24*	68	F	10	52	3
25*	79	M	7	46	3
26*	68	M	10	42	3
27*	65	M	11	40	3
28*	82	F	8	46	4
29	78	F	9	66	4
30	76	M	8	61	4

* indicates the samples used to extract exosomes.

Results

Complement C4 is elevated in PD patients and mouse models

To clarify the role of complement C4 in the pathogenesis of PD, ELISA assays were conducted to measure the levels of complement C4 in plasma and plasma exosomes obtained from PD patients and age-matched controls (Table 1, Fig. 1A). The results revealed a significant elevation of complement C4 in both plasma and exosomes from PD patients compared to controls. Next, western blotting was employed to assess complement C4 levels in the SN of mouse models, including α-syn PFF-injected mice and A53T transgenic mice, alongside respective control groups. The analysis confirmed significantly elevated levels of complement C4 in both α-syn PFF-injected mice and A53T transgenic mice compared to their respective controls (Fig. 1B, C).

To investigate the cellular sources of increased C4 expression in α-syn PFF-injected mice, coronal sections of the substantia nigra from α-syn PFF-injected mice were subjected to dual immunofluorescence staining using markers for activated microglia (IBA1), activated astrocytes (GFAP), neuronal cells (NeuN), and complement C4 (Fig. 1D). The staining revealed higher fluorescence intensity of complement C4 on the α-syn PFF-injected side compared to the non-injected side, indicative of increased complement C4 expression in response to α-synuclein pathology (Fig. 1E). Further co-localization analysis revealed that complement C4 was primarily localized intracellularly within neurons rather than in activated microglia or astrocytes (Fig. 1F–H). These results collectively demonstrate that complement C4 is significantly elevated in PD patients and mouse models of α-synucleinopathy, particularly within neurons, suggesting a potential role in the pathogenesis of PD.

Neuronal secretion of complement C4 induced by α-Syn PFF is amplified by astrocytes

After incubating cell lines with α-syn PFF for 24 h, western blotting analysis was performed to assess complement C4 expression levels. First, western blotting was conducted to examine complement C4 protein expression in BV2 cells, a microglial cell line. There were nearly no levels of C4 protein expression observed in microglia, and α-syn PFF intervention did not alter these levels (Fig. 2A). Similar to microglia, primary astrocytes also didn't exhibit visible levels of complement C4 protein expression, and there was no change in C4 levels after α-syn PFF treatment (Fig. 2B). These findings indicated that BV2 cells and primary astrocytes might not be a primary source of complement C4 induction in response to α-syn PFF. Intriguing, α-syn PFF treatment resulted in a significant increase in complement C4 protein levels compared to the control group treated with PBS in primary cortical neurons (Fig. 2C, D). This suggested that neurons might be a critical cell type responding to α-syn PFF by upregulating complement C4 expression.

To explore the role of astrocytes in modulating complement C4 expression in neurons, a co-culture system was established (Fig. 2E). Neurons were treated with PBS as a negative control, and an equal amount of the same batch of α-syn PFF was separately added to neurons alone and a co-culture of astrocytes and neurons. After 24 h of incubation, cells were harvested and stained with immunofluorescence markers for MAP2, GFAP, and complement C4 (Fig. 2F). The results revealed significantly higher complement C4 fluorescence intensity in the co-culture system compared to neurons cultured alone or in the control group (Fig. 2G). Importantly, complement C4 was predominantly localized in neurons rather than astrocytes within the co-culture system, suggesting that astrocytes may amplify α-syn PFF-induced C4 expression specifically in neurons.

These results collectively demonstrate that α-syn PFF induces an increase in complement C4 expression primarily in neurons rather than in

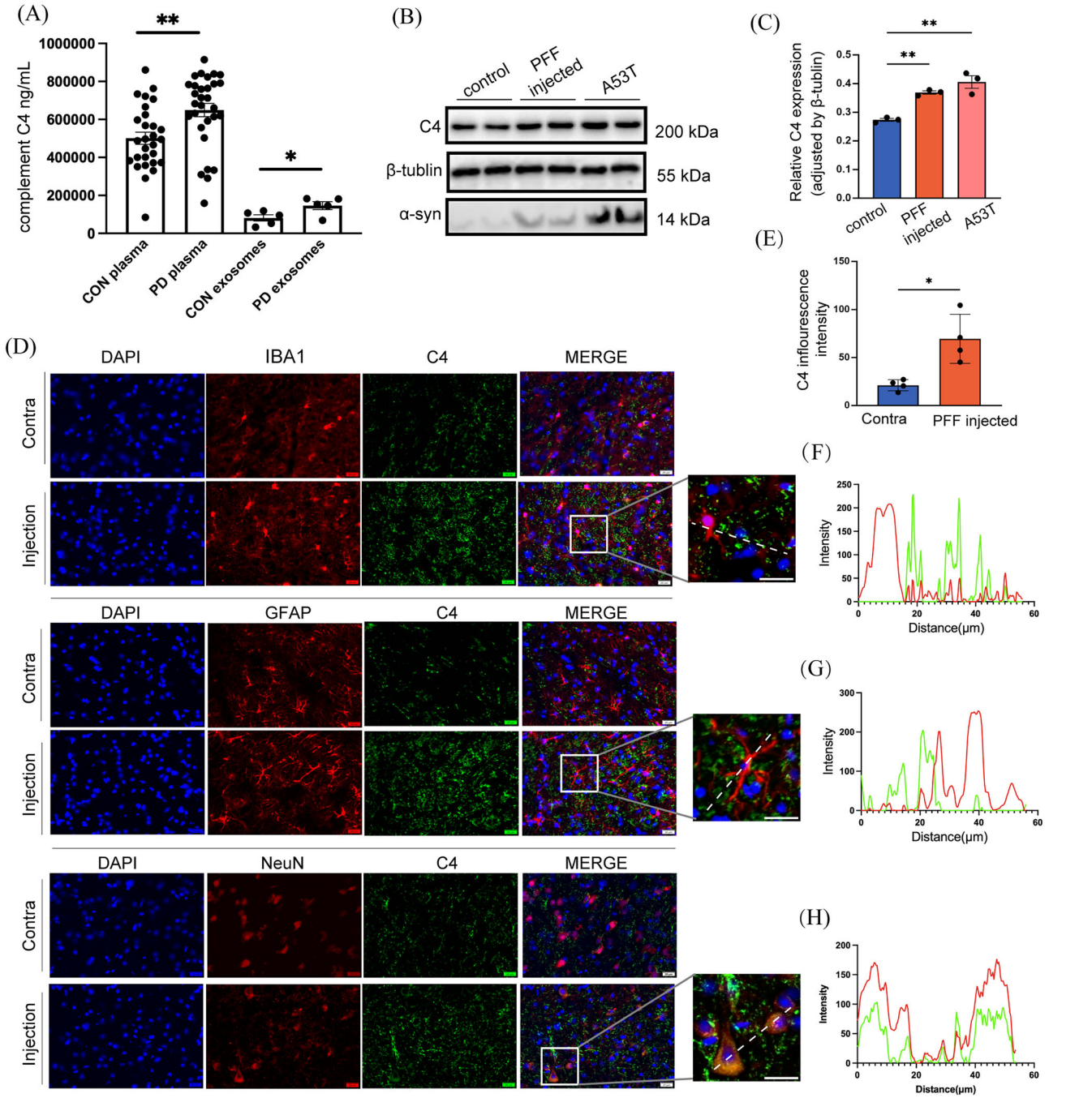

Fig. 1 | Elevated levels of complement C4 in PD patients and mouse models. **A** ELISA results demonstrated elevated levels of Complement C4 in the plasma and exosomes of PD patients. **B** Western blot analysis confirmed increased Complement C4 levels in the SN of α-syn PFF-injected mice and A53T transgenic mice compared to control groups. **C** Quantification of Complement C4 protein levels for each condition in (**B**). PFF-injected mice vs controls, A53T transgenic mice vs controls. **D** Representative images of dual immunofluorescence staining in the SN from α-syn PFF-injected mice, using markers for activated microglia (IBA1), activated astrocytes (GFAP), neuronal cells (NeuN), and Complement C4. Scale bar = 20 μm. **E** The histogram showed quantification of the average optical density of complement C4 on the α-syn PFF-injected side compared to the non-injected side. **F**–**H** Co-localization analysis between microglia, neurons, or astrocytes with complement C4.

microglia or astrocytes. Moreover, the co-culture experiments highlighted that astrocytes enhance C4 expression induced by α-syn PFF specifically within neurons, implicating a potential regulatory role of astrocytes in neuroinflammatory responses mediated by complement activation.

Complement C4 exacerbates astrocytic inflammatory responses, aggravating neuronal damage

To investigate whether C4 can directly promote α-synuclein aggregation in vitro, we incubated α-syn monomers, C4, and a mixture of α-syn monomers with C4 for 72 h, with PBS as the blank control. Every 6 h, we used Thioflavin T staining to assess the aggregation, as the emission spectrum of Thioflavin T shifts to red and its fluorescence intensity increases as the protein aggregates. The fluorescence intensity of the α-syn monomer and C4 mixture was similar to that of the α-syn monomer alone (Supplementary Fig. 2A), and electron microscopy images showed no significant structural differences between the two (Supplementary Fig. 2B). These results suggest that C4 does not directly promote α-syn aggregation in vitro.

To investigate how astrocytes may regulate neuroinflammatory responses through complement activation, cultured mouse cortical astrocytes were treated with α-syn PFF alone, complement C4 alone, α-syn PFF

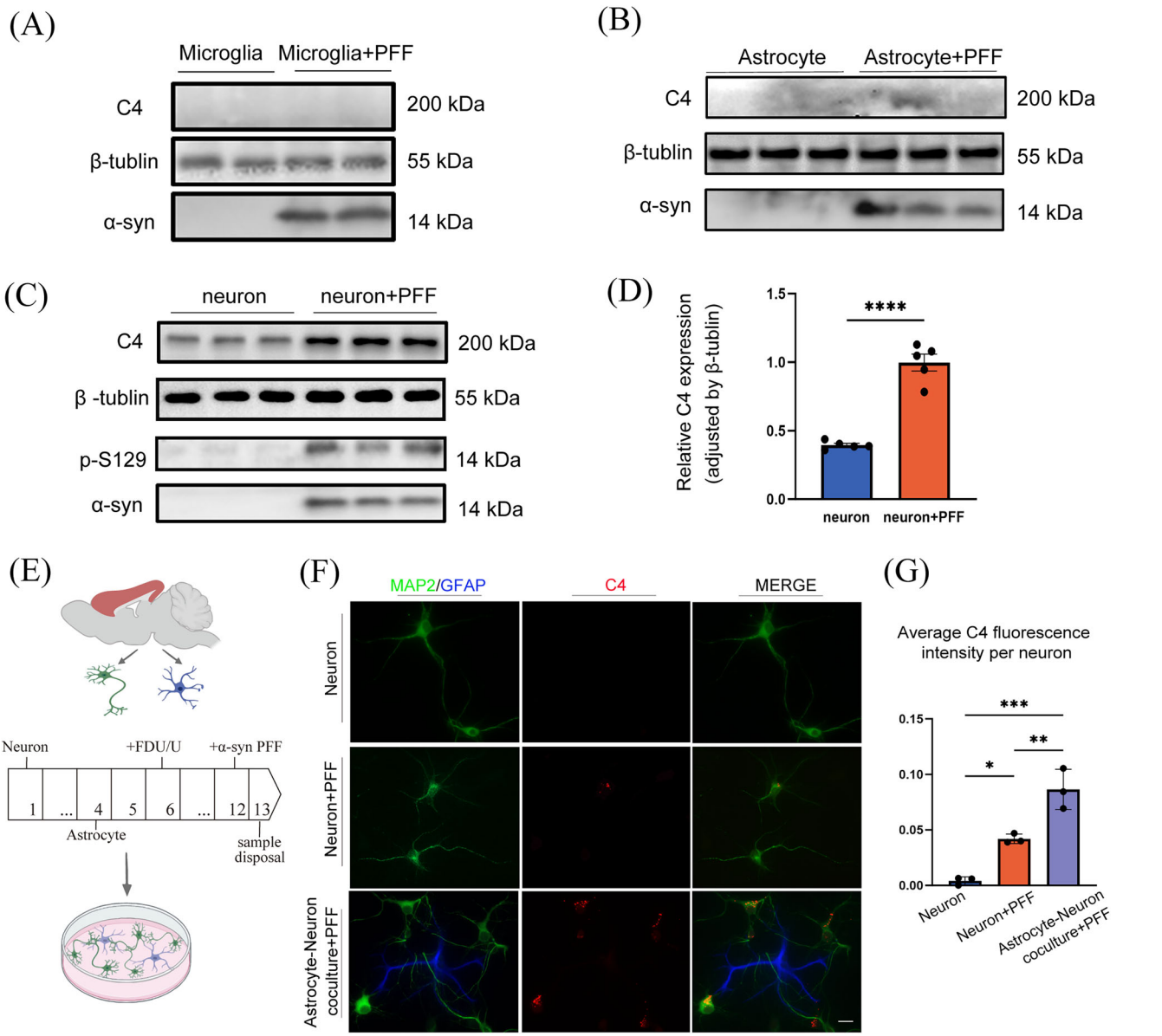

Fig. 2 | α-syn PFF induces neuronal complement C4 expression, enhanced by astrocytes. **A** Western blot analysis showed that complement C4 protein was not expressed in microglial cells before or after α-syn PFF treatment. **B** Western blot analysis revealed no expression of complement C4 protein in primary astrocytes, both before and after α-syn PFF treatment. **C** Western blot analysis demonstrated elevated Complement C4 protein expression in primary cortical neurons after α-syn PFF treatment, compared to PBS-treated controls. **D** Quantification of Complement C4 protein levels for each condition in (**C**). **E** Establishment of a co-culture system comprising astrocytes and neurons to investigate the effects of α-syn PFF. **F** Representative immunofluorescence images showing MAP2, GFAP, and Complement C4 staining in neurons and co-cultures treated with PBS or α-syn PFF. Scale bar = 20 μm. **G** Quantification of average C4 fluorescence intensity per neuron in (**F**).

combined with complement C4 (α-syn PFF + C4), or PBS. Subsequently, the levels of pro-inflammatory cytokines in the cell supernatant were analyzed using ELISA after 3 days. The results revealed that compared to the PBS, C4 and α-syn PFF alone groups, treatment with α-syn PFF + C4 significantly increased the secretion of interleukin-1 beta (IL-1β), interleukin-6 (IL-6), and tumor necrosis factor-alpha (TNF-α) (Fig. 3A). Notably, treatment with C4 alone also resulted in elevated levels of these inflammatory cytokines, but to a lesser extent than the α-syn PFF + C4 condition. Consistent with ELISA findings, qPCR analysis further revealed significant upregulation of IL-1β, IL-6, and TNF-α gene expression in astrocytes treated with α-syn PFF + C4 compared to other treatments, indicating a more robust induction of neuroinflammatory responses (Fig. 3B).

Furthermore, to investigate whether α-syn monomers induce neuroinflammation in astrocytes, we treated astrocytes with PBS, α-syn monomers, C4, and C4 + α-syn monomers. ELISA results (Supplementary Fig. 2C) showed that α-syn monomers did not induce more severe neuroinflammation compared to the control group. In contrast, both the C4 group and the C4 + α-syn monomers group led to high expression of inflammatory factors in astrocytes. However, compared to the C4 alone group, treatment with α-syn monomers + C4 did not significantly increase the secretion of interleukin-1 beta (IL-1β) and tumor necrosis factor-alpha (TNF-α) as seen with α-syn PFF + C4.

These results indicate that complement C4 exacerbates the inflammatory response in astrocytes activated by α-syn PFF, suggesting a potential regulatory role of astrocytes in neuroinflammation through complement activation. A large body of literature indicates that pathological α-syn aggregates (such as α-syn PFF), rather than monomers, are the primary drivers of neuroinflammation and complement activation[20–23]. Therefore, we chose α-syn PFF + C4 for the follow-up experiment.

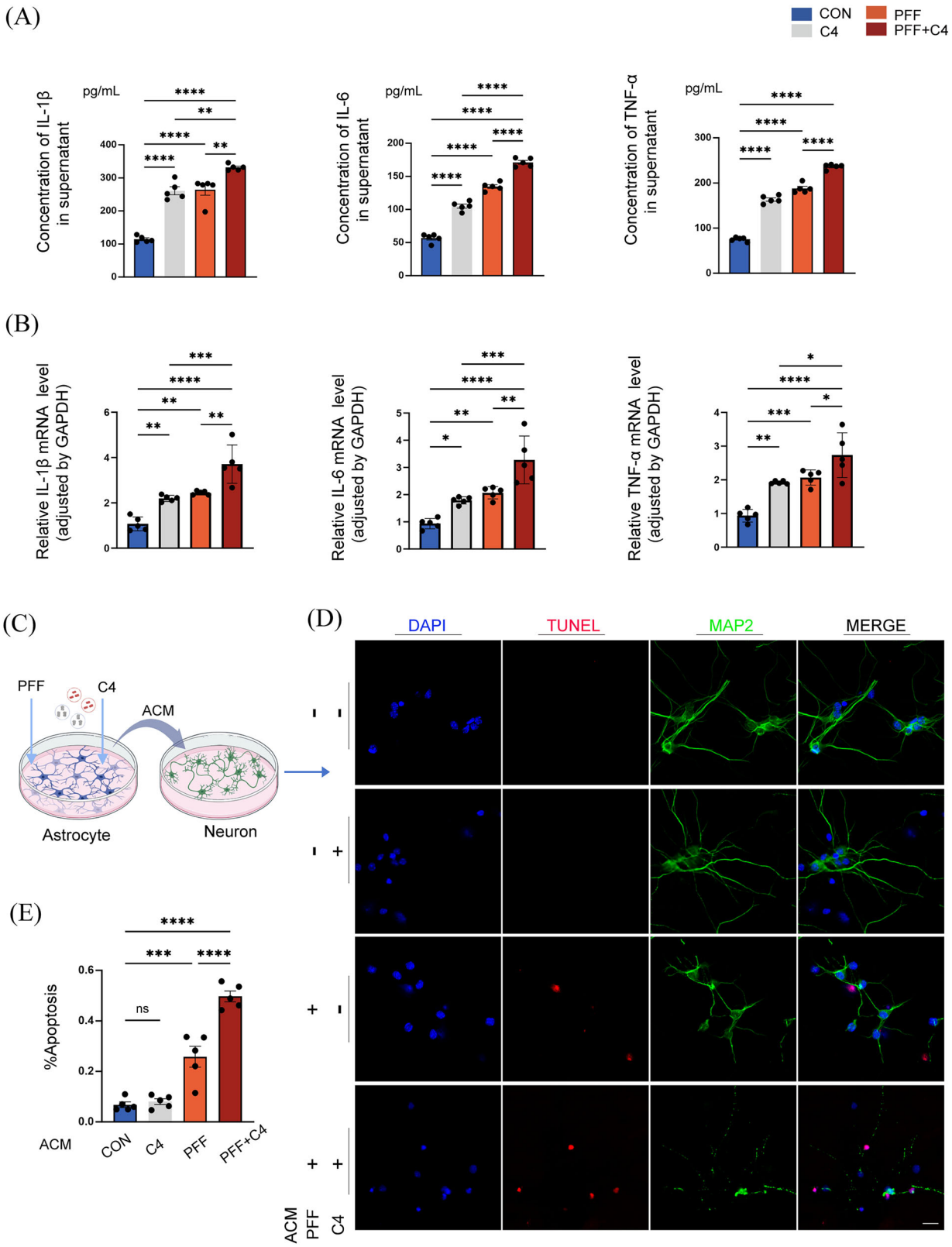

Fig. 3 | Complement C4 exacerbates astrocytic inflammatory responses, aggravating neuronal damage. A In cultured mouse cortical astrocytes, treatment with α-syn PFF, α-syn PFF + C4, C4 alone or PBS was followed by ELISA analysis of pro-inflammatory cytokine levels in the cell supernatant after 3 days. **B** qPCR analysis showed significant upregulation of IL-1β, IL-6, and TNF-α in astrocytes treated with α-syn PFF + C4. **C** Astrocyte-conditioned media (ACM) from different treatments (PBS, C4, α-syn PFF, α-syn PFF + C4) were applied to neurons for 24 h, followed by TUNEL staining to detect apoptotic cells. **D** Harvested cells were subjected to immunofluorescence staining, including TUNEL, MAP2, and DAPI. Scale bar = 20 μm. **E** The histogram showed the ratio of apoptotic neurons to total neurons in the different treatment groups.

To assess the impact of astrocytic inflammatory responses on neurons, astrocyte-conditioned media (ACM) collected from the different treatment conditions (PBS, C4, α-syn PFF, α-syn PFF + C4) was added to neuronal cultures and incubated for 24 h (Fig. 3C). TUNEL staining was performed to detect apoptotic cells as a marker of neuronal damage. Cells were harvested and subjected to immunofluorescence staining, including TUNEL staining for apoptosis, MAP2 staining for neuronal markers, and DAPI staining for nuclear visualization (Fig. 3D). This analysis confirmed that ACM from the α-syn PFF + C4 treatment condition led to a significantly higher proportion of apoptotic neurons compared to ACM from the other treatments (Fig. 3E). Importantly, while C4 treatment alone induced an increase in astrocytic inflammatory factors, it was not sufficient to cause neuronal apoptosis. Taken together, these findings indicate that complement C4 exacerbates astrocytic inflammatory responses induced by α-syn PFF, thereby promoting neuronal damage. The enhanced release of pro-inflammatory cytokines and increased neuronal apoptosis observed in the α-syn PFF + C4 condition highlights the detrimental role of complement C4 in neuroinflammatory processes associated with PD pathology.

Complement C4-treated ACM accelerates α-syn aggregation and synaptic damage in neurons

To investigate the impact of complement C4 on α-syn pathology and synaptic integrity, astrocytes were exposed to interventions with PBS, C4, α-syn PFF, and α-syn PFF+ complement C4. ACM collected from these treatments was then applied to mouse cortical neuron cultures. Immunofluorescence staining for phosphorylated α-synuclein (p-S129 α-syn) and MAP2 was performed at days 3, 6, and 9 post-treatment. The results revealed a progressive increase in pathological α-syn deposition at neuronal synapses over time in neurons exposed to ACM treated with α-syn PFF + C4 (Fig. 4A). Additionally, co-staining of complement C4 and synapsin I (SYN1) in neurons after 24 h showed elevated complement C4 levels closely associated with neuronal damage, as indicated by a significant reduction in SYN1 fluorescence intensity (Fig. 4B). Graphs depicting fluorescence intensities of p-S129 α-syn, C4 and SYN1 further supported these observations (Fig. 4C–E). Notably, C4 treatment did not lead to increased pathological protein expression or more severe neuronal injury compared to the controls. Furthermore, we sequentially extracted TX-100-soluble and TX-100-insoluble proteins from neurons treated as described above. Western blot analysis confirmed these findings, showing increased pathological p-S129 α-syn accumulation and a significant loss of synaptic proteins PSD95 and SYN1 in neurons exposed to ACM from α-syn PFF + C4-treated astrocytes (Fig. 4F–K). Quantification of p-S129 α-syn, as well as PSD95 and SYN1 protein levels, further corroborated these results (Fig. 4F–K).

Immunofluorescence imaging of frozen sections from the substantia nigra of α-syn PFF-injected mice showed co-localization of p-S129 α-synuclein and complement C4, as indicated by white arrows. This in vivo observation supports the association between complement C4 and α-synuclein pathology in a relevant disease model (Fig. 4L).

These findings collectively highlight that ACM treated with α-syn PFF + C4 exacerbates α-synuclein aggregation and induces synaptic damage in neurons. Complement C4 appears to play a critical role in promoting neurodegenerative processes associated with α-synuclein pathology, suggesting a potential mechanism by which astrocytic activation and neuroinflammatory responses contribute to neurodegeneration in α-synuclein-related conditions.

Complement C4 amplifies inflammatory responses and neuronal damage triggered by α-syn PFF in mice

To assess the impact of Complement C4 on neurons and astrocytes in vivo, mice were stereotaxically injected with PBS, complement C4, α-syn PFF, or α-syn PFF + complement C4 into the right striatum. After 3 months post-injection, behavioral assessments were conducted, including the pole test to measure climbing time, the rotarod test for latency to fall, and the hanging test to evaluate motor function. These tests revealed significant impairments in mice injected with α-syn PFF + C4, indicative of exacerbated motor deficits compared to the other three groups (Fig. 5A). Notably, mice injected with C4 alone did not exhibit significant motor impairments compared to the PBS control group.

Immunohistochemistry for tyrosine hydroxylase (TH) in the SN and striatum of the modeled mice showed pronounced dopaminergic neuronal loss in those injected with α-syn PFF + complement C4, compared to the other three groups (Fig. 5B). Statistical analysis confirmed that α-syn PFF + C4 significantly exacerbated dopaminergic neuronal loss in the substantia nigra-striatum pathway (Fig. 5C). However, injection of C4 alone did not lead to substantial dopaminergic neuronal damage, as TH-positive neuron counts remained comparable to control levels.

Analysis of midbrain tissue RNA using qPCR revealed markedly elevated mRNA levels of pro-inflammatory cytokines IL-1β, IL-6, and TNF-α in mice injected with α-syn PFF + complement C4, suggesting heightened neuroinflammatory responses (Fig. 5D). Immunoblotting of midbrain proteins further supported these findings, showing significantly increased levels of IL-1β, IL-6, and TNF-α, along with reduced TH protein levels, indicative of severe neuroinflammation and dopaminergic neuronal damage in α-syn PFF + complement C4-injected mice (Fig. 5E). Together, these results underscore the detrimental impact of complement C4 in exacerbating neuroinflammation and neuronal damage induced by α-syn PFF, highlighting its potential role in the pathogenesis of PD.

Complement C4 exacerbates α-syn aggregation and propagation in mice

Building upon the investigation into complement C4's role in α-syn pathology, fluorescent double labeling of p-S129 α-syn and TH in SN sections of PBS, α-syn PFF, C4, or α-syn PFF + complement C4-injected mice was performed. Subsequent analysis revealed that mice injected with α-syn PFF + complement C4 exhibited heightened pathological α-syn aggregation and more pronounced loss of dopaminergic neurons compared to those injected with PBS, C4 or α-syn PFF alone (Fig. 6A, C). These findings strongly suggest that complement C4 exacerbates α-synuclein aggregation, potentially accelerating neurodegeneration in the context of Parkinson's disease pathology.

Furthermore, immunohistochemistry images of mouse brain sections labeled with p-S129 α-syn demonstrated enhanced pathological α-syn aggregation in critical brain regions including the striatum, substantia nigra, and cortex of PFF + complement C4 model mice (Fig. 6B). These findings suggest that complement C4 contributes to the propagation of α-synuclein pathology across different brain regions, highlighting its role in the amplification of protein aggregation associated with neurodegenerative diseases. Notably, treatment with C4 alone did not result in significant behavioral deterioration, neuronal damage, or pathological protein expression compared to the control group, further supporting the idea that complement C4 acts synergistically with α-syn PFF to exacerbate disease pathology. These findings underscore complement C4's contribution to the propagation of α-syn pathology across different brain regions, emphasizing its role in the amplification of protein aggregation associated with PD.

Discussion

Complement proteins are synthesized locally in the central nervous system (CNS) to maintain immune surveillance, which includes the clearance of pathogens and cellular debris, synaptic pruning, neural circuit refinement, and the maintenance of blood-brain barrier integrity[24]. The involvement of the complement system in the pathogenesis of neurodegenerative diseases has captured our interest. In this study, we investigated the role of complement C4 in the progression of PD, focusing on its impact on neuroinflammation and α-syn pathology. Our results demonstrate that complement C4 is significantly elevated in the plasma of PD patients and SN of PD mouse models induced by α-syn PFF. This increase in complement C4 correlates with exacerbated neuroinflammation, synaptic damage, and neuronal loss, suggesting that C4 plays a critical role in the pathogenesis of PD.

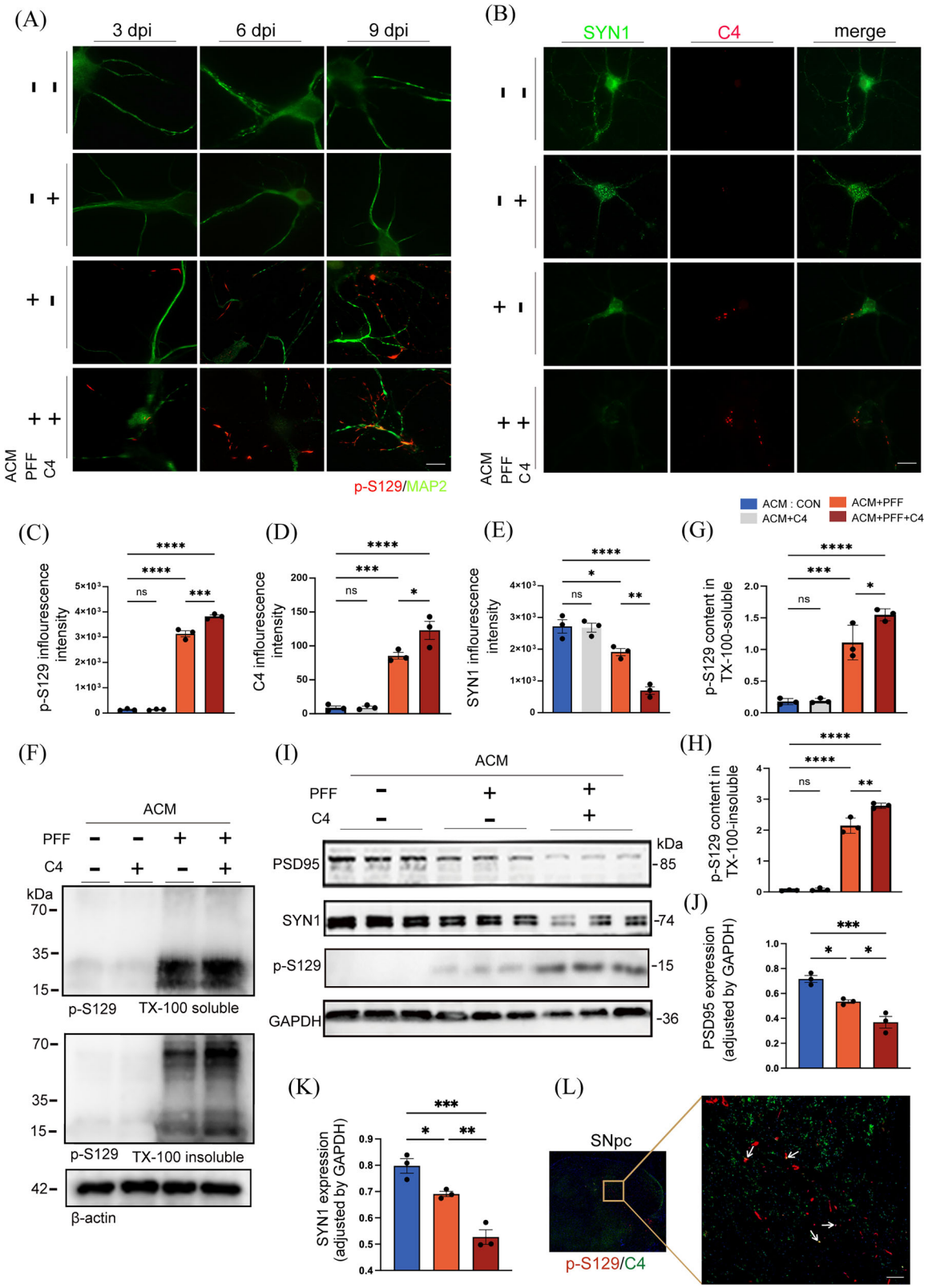

The link between neuroinflammation and neurodegenerative diseases like PD has been increasingly recognized, with microglia and astrocytes playing central roles. Moreover, the crosstalk between the complement system and inflammatory pathways has been widely established[25,26]. Our findings reveal that complement C4 not only acts as a marker of neuroinflammation but also actively contributes to the inflammatory response. In particular, C4 enhances the pro-inflammatory cytokine production by astrocytes in response to α-syn PFF, leading to an amplified inflammatory environment. This heightened inflammation is likely a key factor driving the observed neuronal apoptosis and synaptic loss. The imbalance of the complement system and its involvement in the process of neuroinflammation are often accompanied by an increase in its components.

Fig. 4 | Enhanced α-syn aggregation and synaptic damage in neurons by complement C4-treated ACM. A Following interventions with PBS, C4, α-syn PFF, and α-syn PFF + C4 on astrocytes, ACM was added to mouse cortical neuron cultures. Representative immunofluorescence staining for p-S129 α-syn and MAP2 was performed on neurons at days 3, 6, and 9 post-treatment. Scale bar = 10 μm. **B** Representative images of dual immunofluorescence staining showing complement C4 and neuronal synapsin I (SYN1) in neurons after 24 h of treatment. Scale bar = 10 μm. **C** Quantification of fluorescence intensity for p-S129 from the images in (**A**). **D**, **E** Quantification of fluorescence intensity for C4 and SYN1 from the images in (**B**). **F** Western blot analysis confirmed that ACM treated with α-syn PFF + C4 led to increased expression of both TX-100-soluble and TX-100-insoluble p-S129 α-synuclein. **G**, **H** Quantification of TX-100-soluble or TX-100-insoluble p-S129 syn protein levels for each condition in (**F**). **I** Western blot analysis confirms that treatment of ACM with α-syn PFF + C4 leads to a significant loss of the synaptic proteins PSD95 and SYN1. **J**, **K** Quantification of PSD95, and SYN1 protein levels for each condition in (**I**). **L** Representative immunofluorescence images of frozen sections from the substantia nigra of α-syn PFF-injected mice, labeled for p-S129 α-syn and C4, showing co-localization indicated by white arrows. Scale bar = 50 μm.

Complement components such as C1q and C3, as well as pro-inflammatory cytokines IL-1, IL-6, and TNF-α, were first detected in amyloid plaques of AD patients[27,28]. These cytokines can stimulate the expression of complement components in glial cells or neuroblastoma cell lines to varying degrees[29]. Similarly, activated complement components and cytokines have also been detected near the lesioned areas of the SN in PD patients[10,11]. Toll-like receptors (TLRs) and complement are two components of innate immunity, and many pathogen-associated molecular patterns can simultaneously activate TLRs and complement. Activated complement components C3a and C5a influence signaling pathways such as MAPK and NF-κB by binding to their receptors C3aR and C5aR, thereby regulating TLR signaling and significantly increasing levels of plasma interleukin-6 (IL-6), tumor necrosis factor-alpha (TNF-α), and IL-1β[30]. The terminal product of complement activation, the membrane attack complex (MAC), can induce the activation of inflammatory pathways by increasing intracellular Ca2+ concentration, which accumulates in the mitochondrial matrix, leading to the loss of mitochondrial membrane potential and subsequently triggering the activation of the NLRP3 inflammasome and the release of IL-1β[31,32]. C4 is a key component in the complement activation pathway. Its fragment, C4b, binds with C2a to form the C3 convertase, which mediates the cleavage and activation of C3, subsequently triggering the activation of other complement components, including C5. The addition of exogenous C4 protein to astrocytes may have enhanced this process, leading to an imbalance in the complement system and further activation of glial cells. In total, innate immunity and tissue homeostasis largely depend on properly regulated complement-mediated inflammation. When the complement system is excessively activated or dysregulated, it can lead to the loss of blood-brain barrier integrity and abnormal inflammation, resulting in brain pathology. Dysregulated complement activation, often driven by persistent activating triggers, is responsible for pathological inflammation in many diseases, including neurological disorders.

To investigate the downstream effects of this heightened complement activation, we transferred the conditioned medium from C4-treated astrocytes to primary mouse neurons. Our results showed that these neurons exhibited increased pathological α-syn deposition and more pronounced synaptic marker damage. These findings suggest that C4-mediated neuroinflammation can directly exacerbate neuronal damage and pathological α-syn aggregation. Additionally, we injected a mixture of C4 and α-syn PFF into the unilateral striatum of mice. The results indicated that these mice exhibited more severe neuroinflammation and PD pathological features, including pathological α-syn spread and damage to the nigrostriatal pathway, suggesting that the imbalance of the complement system and the inflammation it mediates can exacerbate the pathological progression of PD. Overall, the imbalance of the complement system, through its interaction with glial cells, amplifies local inflammation, leading to an excessive accumulation of inflammatory factors, and ultimately causing pathological protein aggregation and neuronal damage (Fig. 7).

There is substantial evidence supporting the involvement of complement components in the progression of AD. For instance, amyloid fibrils in AD have been shown to bind to C1q and initiate the classical complement activation pathway, leading to synaptic loss mediated by activated C3b and microglia[33]. Inhibition of key components of this pathway, such as C1q, C3, or the microglial complement receptor CR3, has been shown to reduce early synaptic loss and the number of pro-inflammatory microglia[34]. Furthermore, studies have indicated that knocking out C3, while not preventing Aβ plaque deposition, can alleviate neuroinflammation, slow neurodegeneration, and improve cognitive function in AD models[35]. Similarly, targeting C5aR1, either through gene knockout or pharmacological inhibition, has been shown to reduce amyloid deposition, microglial activation, and behavioral deficits[36,37]. Currently, research on the role of the complement system in the pathogenesis of PD is limited. Our study highlights the critical role of the complement system, particularly complement C4, in the pathogenesis of PD and its potential to exacerbate neuroinflammation and neuronal damage. While the complement system is crucial for maintaining CNS homeostasis, its dysregulation can lead to excessive inflammation, glial activation, and ultimately, neuronal damage.

Together, our results strongly support that the upregulation of complement C4 in PD and its predominant expression by neurons were identified. Using animal models and an astrocyte-neuron co-culture system, C4 was shown to exacerbate neuroinflammation through astrocyte interactions, accelerating PD pathology. Targeting C4 could offer new therapeutic avenues for PD, especially in the context of developing complement system inhibitors.

Methods

Patients and samples

The blood samples used in this study were collected from Union Hospital, Tongji Medical College, Huazhong University of Science and Technology, following approval from the ethics committee. In this study, 30 PD patients (mean age 70.1 ± 6.82 years) and 28 age-matched healthy controls' (mean age 68.1 ± 3.82 years) plasma samples were included. All patients underwent a professional clinical assessment by three neurologists. A diagnosis was established according to the 2015 Movement Disorder Society clinical diagnosis criteria[38]. Furthermore, brain magnetic resonance imaging (MRI), blood biochemical analysis, and other laboratory tests were conducted to rule out secondary parkinsonism. The inclusion criteria for Parkinson's disease (PD) patients were as follows: Age over 55 years; Disease duration of more than 5 years (Table 1). Patients diagnosed with idiopathic PD were clinically assessed for disease severity using the Unified Parkinson's Disease Rating Scale (UPDRS) Part III and the Hoehn & Yahr scale. Healthy control participants were age-matched and had no history of neurological or systemic diseases. None of the participants had a history of cancer, cerebrovascular disease, chronic infectious diseases, or genetic disorders. All participants were fully informed about the study and provided written informed consent before enrollment.

Exosomes were isolated from human plasma and conditioned media using differential centrifugation and ultracentrifugation, following a protocol adapted from Théry et al.[39]. Exosomes were isolated from blood plasma using differential ultracentrifugation. Briefly, plasma samples were first centrifuged at 12,000 × *g* for 45 min to remove cell debris, followed by ultracentrifugation at 110,000 × *g* for 2 h in Beckman Ultra-Clear tubes. The resulting pellet was resuspended in phosphate-buffered saline (PBS), filtered through a 0.22-μm filter, and subjected to a second ultracentrifugation at 110,000 × *g* for 70 min to further purify the exosomes. The final pellet was resuspended in PBS and stored at −80 °C for further analysis. All centrifugation steps were performed at 4 °C.

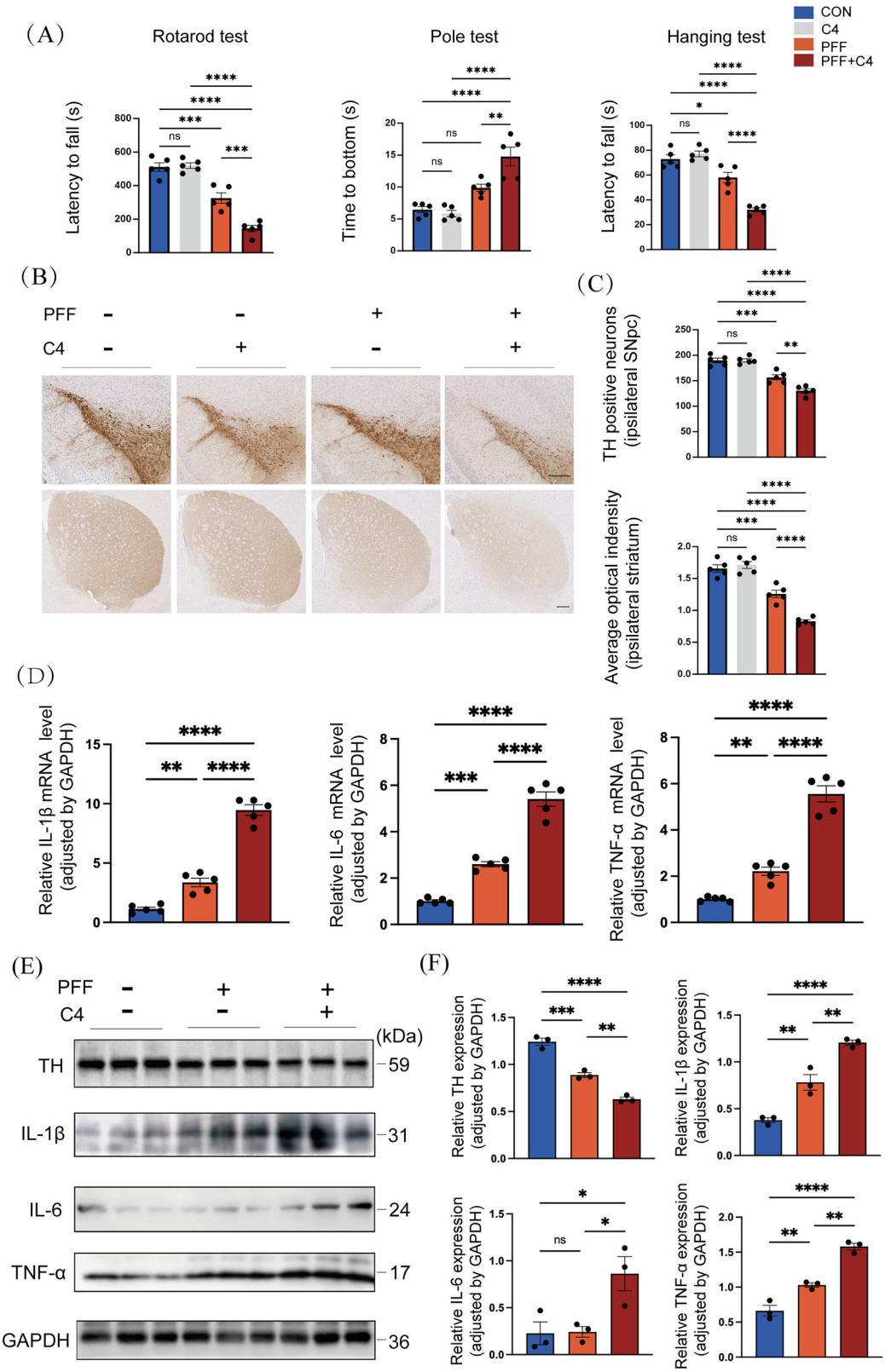

Fig. 5 | Complement C4 exacerbates inflammation and neuronal damage in vivo. **A** Mice were stereotactically injected with α-syn PFF, C4, α-syn PFF + C4, or PBS into the right striatum. Behavioral tests, including pole climbing, rotarod performance, and hanging test, were conducted after 3 months to assess motor function. **B** TH immunohistochemistry was performed on the substantia nigra and striatum. Scale bar = 200 μm. **C** Statistical analysis showed increased dopaminergic neuronal loss in the substantia nigra-striatum pathway with α-syn PFF + C4 treatment. **D** qPCR analysis of midbrain tissue showed elevated mRNA levels of IL-1β, IL-6, and TNF-α with α-syn PFF + C4 treatment. **E** Immunoblotting demonstrated higher protein levels of IL-1β, IL-6, and TNF-α, as well as reduced TH levels in midbrain tissue following α-syn PFF + C4 injection. **F** Quantification of TH, IL-1β, IL-6, and TNF-α protein levels for each condition in (**E**).

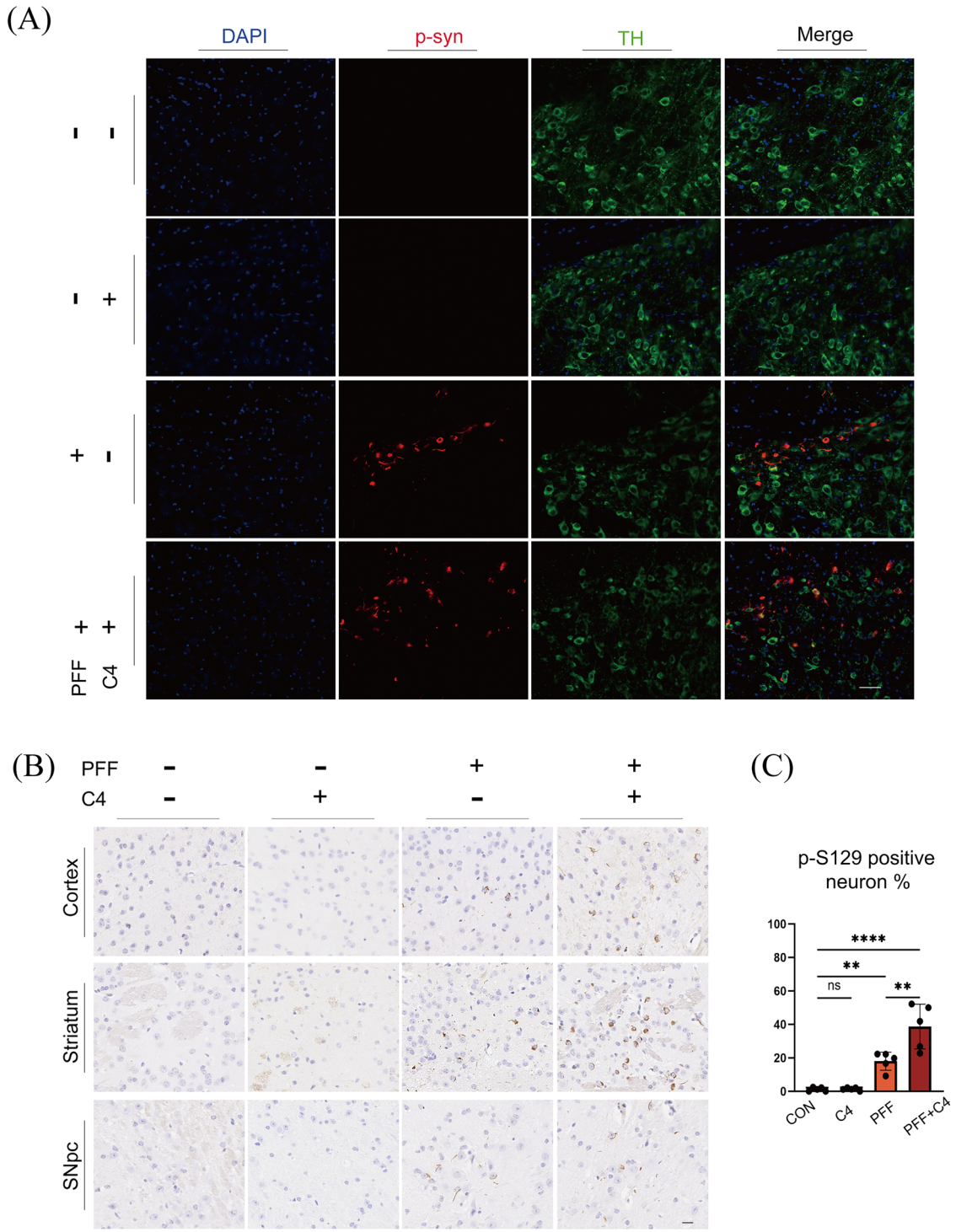

Fig. 6 | Complement C4 exacerbates α-syn aggregation and propagation in vivo. **A** Representative fluorescent double labeling of p-S129 α-syn and TH in SN sections from mice injected with PBS, C4, α-syn PFF, or α-syn PFF + complement C4. Scale bar = 50 μm. **B** Representative Immunohistochemistry images of mouse brain sections labeled with p-S129 α-syn. Scale bar = 50 μm. **C** Quantification of the percentage of p-S129-positive neurons in the ipsilateral SN.

Preparation of α-syn PFF

α-Synuclein (α-syn) monomers were thawed on ice and diluted with PBS to a final concentration of 2 mg/mL. The mixture was vortexed and transferred into sterile, enzyme-free centrifuge tubes, with tube caps sealed using parafilm. The tubes were placed in a temperature-controlled shaker (37 °C, 1000 RPM) and shaken continuously for 7 days. After shaking, turbid α-syn preformed fibrils (PFF) were formed. The purified protein solution was stored at −80 °C until use. Prior to experiments, α-syn PFF were sonicated in a water bath for 15 min. Transmission electron microscopy (TEM) negative staining experiments were used to verify the success of α-syn PFF preparation, which service was provided by Wuhan Servicebio Technology CO.,LTD. The images obtained by TEM were supplemented in Supplementary Fig. 1, including before and after α-syn PFF was sonicated.

Stereotactic injection

For stereotactic injections, α-syn PFF were prepared at a final concentration of 2 μg/μL and sonicated using an ultrasonic cell disruptor. For the α-syn PFF + C4 mixture, exogenous complement C4 protein was added to the

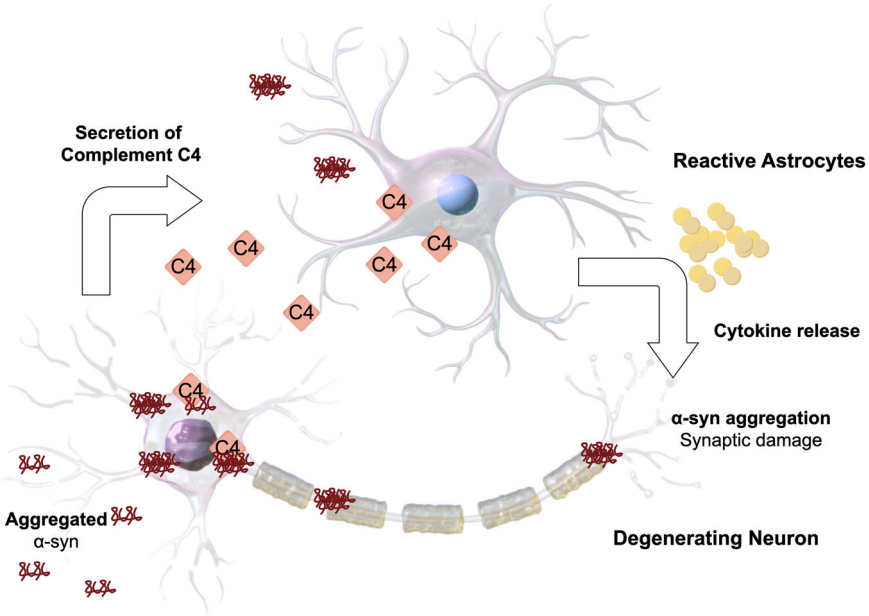

Fig. 7 | Role of complement C4 in α-syn aggregation and neuroinflammation. Aggregated α-syn leads to the secretion of complement C4 by neurons, resulting in increased levels of complement C4 around astrocytes. The activation of astrocytes also triggers the release of pro-inflammatory cytokines, further exacerbating α-syn aggregation and neuronal damage. This pathway highlights the role of complement C4 in α-syn aggregation and neuroinflammation in PD.

sonicated α-syn PFF solution (2 μg/μL) at a final concentration of 1 μg/μL, followed by thorough mixing. All animal experimental protocols were approved by the Animal Care and Use Committee of Huazhong University of Science and Technology. Two-month-old male C57BL/6 mice (25 ± 1.5 g) were anesthetized via intraperitoneal injection of 250 μL 5% chloral hydrate. The scalp hair was shaved, and the head was fixed in a stereotaxic apparatus (RWD). After disinfection with iodine, a midline incision was made along the skull. The fascia was cleaned with hydrogen peroxide, and the bregma and lambda were exposed and marked. A microsyringe (Hamilton) was mounted onto the stereotaxic frame, and the skull was adjusted to a horizontal position using bregma and lambda as reference points. Using bregma as the origin, a small craniotomy was drilled at coordinates X = +2.05 mm, Y = +0.30 mm. The microsyringe was slowly lowered to Z = −2.80 mm, and after a 10-min stabilization period, 5 μL of the prepared solution was injected at a slow rate. The needle was left in place for an additional 10 min to minimize backflow and then withdrawn slowly. The scalp was sutured, and the wound was treated with lidocaine (analgesic) and lincomycin (antibiotic). Mice were monitored post-surgery until full recovery and housed for 3 months before further analysis.

Mouse brain tissue protein extraction

Mouse brain regions (cortex, substantia nigra, striatum, and cerebellum) were isolated on ice. The tissues were weighed and transferred into homogenization tubes. Protein lysis buffer containing RIPA lysis buffer (Beyotime), phosphatase inhibitors (Servicebio), PMSF (Servicebio), and protease inhibitor cocktail (Servicebio) was added at a ratio of 10 μL per 1 mg tissue, followed by the addition of 2 magnetic beads. Homogenization was performed using a homogenizer (6500 RPM, 4 °C, 30 sec). After removing the magnetic beads, tissues were lysed on ice for 30 min and further disrupted using an ultrasonic cell disruptor (30% power, 2 s on/1 sec off, 5 cycles). The lysates were centrifuged (12,000 × *g*, 5 min, 4 °C), and the supernatants containing the extracted proteins were collected and stored at −80 °C for subsequent experiments.

RNA extraction and real-time PCR

Brain tissues were weighed and transferred into 2 mL grinding tubes. For every 100 mg tissue, 1 mL RNA isolator (Vazyme R401) and 2 zirconium oxide beads were added. Tissues were homogenized (60 Hz, 4 °C, 3 min) until no visible fragments remained. After bead removal, samples were centrifuged (11,200 rpm, 5 min, 4 °C). The supernatant was transferred to a new tube, mixed with 1/5 volume chloroform, and vigorously shaken until the solution turned milky. After incubation on ice, samples were centrifuged (11,200 rpm, 15 min, 4 °C). The upper aqueous phase was carefully collected, mixed with an equal volume of pre-cooled isopropanol, and incubated on ice for 10 min. Following centrifugation (11,200 rpm, 5 min, 4 °C), the RNA pellet was washed with 1 mL 75% ethanol, air-dried, and dissolved in RNase-free water. RNA concentration and purity were measured using a spectrophotometer.

The culture medium was removed, and cells were washed once with PBS. 1 mL RNA isolator (Vazyme R401) was added per well of a 6-well plate, ensuring complete cell coverage. Cells were detached using a cell scraper, transferred to 1.5 mL tubes, and lysed by repeated pipetting. Total RNA was extracted using TRIzol reagent (Takara 9109). cDNA synthesis was performed via reverse transcription, and real-time PCR was conducted using a StepOnePlus system (Applied Biosystems).

Western blot analysis

Mouse brain tissue or cell lysates were prepared using RIPA lysis buffer supplemented with phosphatase inhibitors, protease inhibitor cocktail, and PMSF. Protein samples were separated by 7.5–15% SDS-PAGE and subsequently transferred onto nitrocellulose membranes (Millipore). The membranes were blocked with 5% BSA for 1 h at room temperature, followed by overnight incubation at 4 °C with the following primary antibodies: anti-C4 (Hycult Biotech, HM1046-20UG, 1:500), anti-α-syn (GeneTex, GTX112799, 1:1000), anti-phosphorylated-S129 (Biolegend, 825702, 1:500), anti-β-tubulin (Proteintech, 10094-1-AP, 1:10000), anti-SYN1 (Proteintech, 20258-1-AP, 1:500), anti-PSD95 (Proteintech, 30255-1-AP, 1:500), anti-TH (Proteintech, 25859-1-AP,1:1000), anti-IL-1β (Abcam, ab234437, 1:1000), anti-TNF-α (Cell Signaling Technology, 11948, 1:1000), anti-IL-6 (Cell Signaling Technology, 12912, 1:1000), and anti-GAPDH (Proteintech, 10494-1-AP, 1:5000). After washing, membranes were incubated with appropriate HRP-conjugated secondary antibodies for 1 h at room temperature. Protein bands were visualized using enhanced chemiluminescence reagent and quantified using ImageJ software (NIH).

Immunofluorescence (IF) staining

Immunofluorescence staining was performed on frozen mouse brain sections. The sections were permeabilized with 0.5% Triton X-100 for 30 min and then blocked with 5% BSA for 30 min. The sections were incubated overnight at 4 °C with primary antibodies. The brain sections were then

incubated with secondary antibodies conjugated to Alexa Fluor 488 or 594 for 1 h. The nuclei were stained with 4′,6-diamidino-2-phenylindole (DAPI). Imaging of the sections was carried out using a fluorescence microscope (Olympus). Primary astrocytes or neurons were cultured on coverslips and treated as required. The cells were fixed with 4% paraformaldehyde and stained according to the procedure described for the frozen brain sections. The following primary antibodies were used: C4 (Hycult Biotech, HM1046-20UG, 1:100), IBA1 (Abcam, ab178846, 1:200), GFAP (Proteintech, 60190-1-Ig, 1:100), NeuN (Proteintech, 26975-1-AP, 1:100), TH (Proteintech, 25859-1-AP, 1:200), MAP2 (Abcam, ab5392, 1:1000), phosphorylated-S129 (Biolegend, 825702, 1:100) and SYN1 (Proteintech, 20258-1-AP, 1:100).

Immunohistochemistry (IHC)

Paraffin-embedded sections were deparaffinized and rehydrated. After antigen retrieval with citrate antigen retrieval solution (pH 6.0), endogenous peroxidase was inactivated with 3% hydrogen peroxide. The subsequent steps are identical to those in IF staining, up until the use of HRP-conjugated secondary antibodies. After the diaminobenzidine (DAB) reaction, the nuclei were stained with hematoxylin. The following primary antibody was used: TH (25859-1-AP, Proteintech) and phosphorylated-S129 (Biolegend).

Isolation and culture of primary mouse astrocytes

T75 culture flasks (Corning) were coated with 50 μg/mL poly-L-lysine (biosharp) for 1 h at room temperature, followed by three PBS washes and drying in a 37 °C incubator. Complete culture medium was prepared by supplementing DMEM-F12 (Gibco) with 10% FBS (Celligent) and 1% penicillin-streptomycin (biosharp), then preheated to 37 °C. One-day-old mouse pups were disinfected with 70% ethanol and decapitated. The skull was bisected along the midline to expose the brain, which was immediately transferred to pre-cooled DMEM-F12. Under a stereomicroscope (OLYMPUS), the olfactory bulbs and cerebellum were removed, followed by careful meningeal and vascular stripping from cortical tissue to minimize contamination. The isolated cortex was transferred to a fresh dish containing 3 mL pre-cooled DMEM-F12 and mechanically dissociated into ~1 mm^3 fragments. Tissue digestion was performed using 1 mL of 5% trypsin (Gibco) at 37 °C for 15 min, with gentle trituration every 5 min. The enzymatic reaction was terminated by adding an equal volume of complete medium. The cell suspension was filtered through a 40 μm mesh and centrifuged (1000 rpm, 4 °C, 5 min). The pelleted cells were resuspended in complete medium and seeded into prepared T75 flasks at a density of $10–15 \times 10^6$ cells per flask. Medium was replaced on day 2 and subsequently every 3 days. At confluence (days 7–8), microglial cells were removed by shaking (180 rpm, 30 min). Following supernatant removal, 20 mL fresh medium was added, and flasks were shaken vigorously (240 rpm, 6 h) to eliminate oligodendrocyte precursor cells. The remaining adherent cells represented purified astrocytes, which were maintained until reaching maturity (days 21–28) for experimental use.

Isolation and culture of primary mouse neurons

Six-well plates (NEST) and 14 mm coverslips (biosharp) were coated with 50 μg/mL poly-L-lysine (biosharp) for 1 h at room temperature, followed by three PBS washes and drying in a 37 °C incubator. Complete culture medium (prepared as previously described) and neuron culture medium (Neurobasal [Gibco] supplemented with 1% penicillin-streptomycin [biosharp], 1% glutamine [Gibco], and 2% B27 supplement [Gibco]) were preheated to 37 °C. Primary neurons were isolated from postnatal day 0–1 mouse pups using the cortical dissection protocol previously described. The cell suspension was centrifuged (1000 rpm, 4 °C, 5 min), and the supernatant was discarded. The pellet was resuspended in complete medium and cell density was determined using a hemocytometer (MARIENFELD). Cells were seeded at densities of 8×10^5 cells per well for coverslip cultures or 2×10^6 cells per well for protein extraction experiments. After 6 h of incubation, cell attachment was verified by microscopic examination. The complete medium was then replaced with neuron culture medium. Half-medium changes were performed every 3 days, and cultures were maintained for up to 4 weeks in vitro.

Neuron-astrocyte co-culture system

The co-culture system was established according to methods described in the literature[40–42].

Day 1: Cortical mixed cells were isolated from neonatal mice and seeded in a T75 culture flask (as previously described).

Day 4: Cortical neurons were isolated from neonatal mice (as previously described). The neurons were resuspended in the neuron culture medium and the cell density was adjusted to 4×10^5 cells/mL. 2 mL of this suspension was added to each well of a six - well plate, so that 8×10^5 neurons were present per well.

Day 7: 1.9 mL of medium was removed from each well and 1.4 mL of fresh neuron culture medium was added, leaving 1.5 mL of neuron culture medium per well. Astrocytes were purified from the T75 flask (as previously described), resuspended in a complete medium, and the cell density was adjusted to 6.4×10^5 cells/mL. 0.5 mL of this astrocyte suspension was added to each well of the six - well plate, resulting in a neuron - to - astrocyte ratio of 5:2.

Day 9: A half medium change was performed with neuron culture medium, and 5 - fluoro - 2'-deoxyuridine (FdU) and uridine were added to each well, achieving final concentrations of 8 μg/mL and 28 μg/mL, respectively, to inhibit excessive glial cell proliferation.

After this, half medium changes were performed with neuron culture medium every three days, cell morphology was monitored, and interventions were applied as needed.

Sequential extraction

Primary cortical neurons were lysed in three-phase buffered saline (TBS) (Servicebio) containing 1% TX-100 (Sigma), protease and phosphatase inhibitors. The mixture was mechanically homogenized, sonicated and centrifuged at $100,000 \times g$ for 1 h (4 °C). The supernatant was collected as TX-100-soluble content. The precipitate was resuspended with the same buffer as above, sonicated and centrifuged at $100,000 \times g$ for 1 h at 4 °C. Then, the precipitate was resuspended in TBS buffer containing 2% sodium dodecyl sulfate, sonicated and centrifuged at $100,000 \times g$ for 1 h at room temperature. The supernatant is collected as TX-100-insoluble content.

ELISA analysis

The blood samples used in this study were collected from Union Hospital, Tongji Medical College, Huazhong University of Science and Technology, following approval from the ethics committee. In this study, 30 PD patients and 28 age-matched healthy controls' plasma samples were included. All patients underwent a professional clinical assessment by three neurologists. A diagnosis was established according to the 2015 Movement Disorder Society clinical diagnosis criteria[38]. Exosomes were isolated from human plasma and conditioned media using differential centrifugation and ultracentrifugation, following a protocol adapted from Théry et al.[39]. Plasma C4 levels and plasma exosomal C4 levels were quantified using a human C4 ELISA kit (Elabscience), following the manufacturer's protocol.

Levels of specific inflammatory cytokines, including IL-1β, TNF-α, and IL-6, were quantified in the supernatant of primary astrocyte cultures using ELISA (Elabscience). The assay was conducted following the manufacturer's instructions to accurately measure the concentration of these cytokines in the cell culture supernatant.

Behavioral test

Rotarod Test: Prior to formal testing, mice were acclimated to the rotarod apparatus through a 3-day training protocol consisting of daily 10-minute sessions at a fixed speed of 20 rpm to minimize anxiety-related behaviors and accidental falls. For the formal assessment, the rotarod was programmed to accelerate to a maximum speed of 40 rpm. The latency to fall was recorded for each trial, with a maximum cutoff time of 10 min. Each animal underwent three test trials separated by 1-h inter-trial intervals.

Pole Test: A vertical pole (1 cm diameter × 50 cm height) with a rough surface texture was positioned in the home cage. Mice were gently placed atop the pole on a rubber platform, and the time required to descend to the base of the pole was recorded. Three trials were conducted per animal with 10-minute rest periods between trials.

Hanging Test: A horizontal metal wire (1.5 mm diameter) was suspended above the home cage. Mice were positioned with their forepaws grasping the wire, and the duration of maintained grip was recorded until exhaustion-induced falling occurred. Three trials were performed per animal with 10-minute recovery periods between tests.

Statistical analysis

All data are presented as means ± SEMs from three or more independent samples. Statistical analysis and graphing were performed using GraphPad Prism. An independent t-test was used for comparisons between two groups, while one-way ANOVA was applied for multiple group comparisons. A p-value of <0.05 was considered statistically significant ($^{*}p < 0.05$; $^{**}p < 0.01$; $^{***}p < 0.001$; $^{****}p < 0.0001$).

Data availability

All relevant data generated during this study are available from the corresponding author on reasonable request.

Received: 9 February 2025; Accepted: 21 May 2025;
Published online: 28 May 2025

References

1. Ricklin, D., Hajishengallis, G., Yang, K. & Lambris, J. D. Complement: a key system for immune surveillance and homeostasis. *Nat. Immunol.* **11**, 785–797 (2010).
2. Okuzumi, A. et al. Propagative alpha-synuclein seeds as serum biomarkers for synucleinopathies. *Nat. Med.* **29**, 1448–1455 (2023).
3. Tansey, M. G. et al. Inflammation and immune dysfunction in Parkinson disease. *Nat. Rev. Immunol.* **22**, 657–673 (2022).
4. Wang, Y. et al. Complement 3 and factor h in human cerebrospinal fluid in Parkinson's disease, Alzheimer's disease, and multiple-system atrophy. *Am. J. Pathol.* **178**, 1509–1516 (2011).
5. Vesely, B. et al. Interleukin 6 and complement serum level study in Parkinson's disease. *J. Neural Transm.* **125**, 875–881 (2018).
6. Naskar, A. et al. Fibrinogen and complement factor H are promising CSF protein biomarkers for Parkinson's disease with cognitive impairment horizontal line A proteomics-ELISA-based study. *ACS Chem. Neurosci.* **13**, 1030–1045 (2022).
7. Winchester, L. et al. Identification of a possible proteomic biomarker in Parkinson's disease: discovery and replication in blood, brain and cerebrospinal fluid. *Brain Commun.* **5**, fcac343 (2023).
8. Togo, T. et al. Glial involvement in the degeneration process of Lewy body-bearing neurons and the degradation process of Lewy bodies in brains of dementia with Lewy bodies. *J. Neurol. Sci.* **184**, 71–75 (2001).
9. Depboylu, C. et al. Possible involvement of complement factor C1q in the clearance of extracellular neuromelanin from the substantia nigra in Parkinson disease. *J. Neuropathol. Exp. Neurol.* **70**, 125–132 (2011).
10. Loeffler, D. A., Camp, D. M. & Conant, S. B. Complement activation in the Parkinson's disease substantia nigra: an immunocytochemical study. *J. Neuroinflammation* **3**, 29 (2006).
11. Yamada, T., McGeer, P. L. & McGeer, E. G. Lewy bodies in Parkinson's disease are recognized by antibodies to complement proteins. *Acta Neuropathol.* **84**, 100–104 (1992).
12. Gregersen, E. et al. Alpha-synuclein activates the classical complement pathway and mediates complement-dependent cell toxicity. *J. Neuroinflammation* **18**, 177 (2021).
13. Juul-Madsen, K. et al. Size-selective phagocytic clearance of fibrillar alpha-synuclein through conformational activation of complement receptor 4. *J. Immunol.* **204**, 1345–1361 (2020).
14. Jing, L. et al. Microglial activation mediates noradrenergic locus coeruleus neurodegeneration via complement receptor 3 in a rotenone-induced Parkinson's disease mouse model. *J. Inflamm. Res* **14**, 1341–1356 (2021).
15. Liang, Y. et al. Complement 3-deficient mice are not protected against MPTP-induced dopaminergic neurotoxicity. *Brain Res.* **1178**, 132–140 (2007).
16. Depboylu, C. et al. Upregulation of microglial C1q expression has no effects on nigrostriatal dopaminergic injury in the MPTP mouse model of Parkinson disease. *J. Neuroimmunol.* **236**, 39–46 (2011).
17. Gallego, J. A., Blanco, E. A., Morell, C., Lencz, T. & Malhotra, A. K. Complement component C4 levels in the cerebrospinal fluid and plasma of patients with schizophrenia. *Neuropsychopharmacology* **46**, 1140–1144 (2021).
18. Zhou, J. et al. Cerebrospinal Fluid Complement 4 Levels Were Associated with Alzheimer's Disease Pathology and Cognition in Non-Demented Elderly. *J. Alzheimers Dis.* **96**, 1071–1081 (2023).
19. Sellgren, C. M. et al. Increased synapse elimination by microglia in schizophrenia patient-derived models of synaptic pruning. *Nat. Neurosci.* **22**, 374–385 (2019).
20. Ma, S. X. et al. Complement and coagulation cascades are potentially involved in dopaminergic neurodegeneration in alpha-synuclein-based mouse models of Parkinson's disease. *J. Proteome Res* **20**, 3428–3443 (2021).
21. Yang, Y. et al. Complement receptor 1 is a potential extracerebral factor promoting alpha-synuclein pathology. *Mol. Neurobiol.* **62**, 4605–4616 (2025).
22. Hinkle, J. T. et al. STING mediates neurodegeneration and neuroinflammation in nigrostriatal alpha-synucleinopathy. *Proc. Natl Acad. Sci. USA* **119**, e2118819119 (2022).
23. Hong, H. et al. Suppression of the JAK/STAT pathway inhibits neuroinflammation in the line 61-PFF mouse model of Parkinson's disease. *J. Neuroinflammation* **21**, 216 (2024).
24. Schartz, N. D. & Tenner, A. J. The good, the bad, and the opportunities of the complement system in neurodegenerative disease. *J. Neuroinflammation* **17**, 354 (2020).
25. Jane-wit, D. et al. Complement membrane attack complexes activate noncanonical NF-kappaB by forming an Akt+ NIK+ signalosome on Rab5+ endosomes. *Proc. Natl Acad. Sci. USA* **112**, 9686–9691 (2015).
26. Mastellos, D. C., Hajishengallis, G. & Lambris, J. D. A guide to complement biology, pathology and therapeutic opportunity. *Nat. Rev. Immunol.* **24**, 118–141 (2024).
27. Eikelenboom, P. & Stam, F. C. Immunoglobulins and complement factors in senile plaques. An immunoperoxidase study. *Acta Neuropathol.* **57**, 239–242 (1982).
28. Stoltzner, S. E. et al. Temporal accrual of complement proteins in amyloid plaques in Down's syndrome with Alzheimer's disease. *Am. J. Pathol.* **156**, 489–499 (2000).
29. Veerhuis, R. et al. Cytokines associated with amyloid plaques in Alzheimer's disease brain stimulate human glial and neuronal cell cultures to secrete early complement proteins, but not C1-inhibitor. *Exp. Neurol.* **160**, 289–299 (1999).
30. Zhang, X. et al. Regulation of toll-like receptor-mediated inflammatory response by complement in vivo. *Blood* **110**, 228–236 (2007).
31. Triantafilou, K., Hughes, T. R., Triantafilou, M. & Morgan, B. P. The complement membrane attack complex triggers intracellular Ca2+ fluxes leading to NLRP3 inflammasome activation. *J. Cell Sci.* **126**, 2903–2913 (2013).
32. Morgan, B. P. The membrane attack complex as an inflammatory trigger. *Immunobiology* **221**, 747–751 (2016).
33. Tacnet-Delorme, P., Chevallier, S. & Arlaud, G. J. Beta-amyloid fibrils activate the C1 complex of complement under physiological conditions: evidence for a binding site for A beta on the C1q globular regions. *J. Immunol.* **167**, 6374–6381 (2001).

34. Hong, S. et al. Complement and microglia mediate early synapse loss in Alzheimer mouse models. *Science* **352**, 712–716 (2016).
35. Shi, Q. et al. Complement C3 deficiency protects against neurodegeneration in aged plaque-rich APP/PS1 mice. *Sci. Transl. Med.* **9**, https://doi.org/10.1126/scitranslmed.aaf6295 (2017).
36. Hernandez, M. X. et al. Prevention of C5aR1 signaling delays microglial inflammatory polarization, favors clearance pathways and suppresses cognitive loss. *Mol. Neurodegener.* **12**, 66 (2017).
37. Fonseca, M. I. et al. Treatment with a C5aR antagonist decreases pathology and enhances behavioral performance in murine models of Alzheimer's disease. *J. Immunol.* **183**, 1375–1383 (2009).
38. Postuma, R. B. et al. MDS clinical diagnostic criteria for Parkinson's disease. *Mov. Disord.* **30**, 1591–1601 (2015).
39. Thery, C., Amigorena, S., Raposo, G. & Clayton, A. Isolation and characterization of exosomes from cell culture supernatants and biological fluids. *Curr. Protoc. Cell Biol.* https://doi.org/10.1002/0471143030.cb0322s30 (2006).
40. Goshi, N., Morgan, R. K., Lein, P. J. & Seker, E. A primary neural cell culture model to study neuron, astrocyte, and microglia interactions in neuroinflammation. *J. Neuroinflammation* **17**, 155 (2020).
41. Wasilewski, D. et al. Reactive astrocytes contribute to Alzheimer's disease-related neurotoxicity and synaptotoxicity in a neuron-astrocyte co-culture assay. *Front. Cell Neurosci.* **15**, 739411 (2021).
42. Oh, H. N. et al. In vitro neurotoxicity evaluation of biocidal disinfectants in a human neuron-astrocyte co-culture model. *Toxicol. Vitr.* **84**, 105449 (2022).

Acknowledgements

This work was supported by grants 82471456 and 82101338 from the National Natural Science Foundation of China (to Y.X.), and grant 82171424 from the National Natural Science Foundation of China (to T.W.).

Author contributions

Y.X. and T.W. conceived the experiments and revised the manuscript. W.K.Z. performed most of the experiments and drafted the manuscript. Y.M.W. was involved in the in vivo experiments. L.K. and Z.J.J. helped in the in vitro experiments. L.K. and N.X. were involved in data analysis. All authors read and approved the final manuscript.

Competing interests

The authors declare no competing interests.

Additional information

Supplementary information The online version contains supplementary material available at https://doi.org/10.1038/s41531-025-01005-z.

Correspondence and requests for materials should be addressed to Tao Wang or Yun Xia.